A Statistical Analysis of the Effect of Substrate Utilization and Shear Stress on the Kinetics of Biofilm Detachment

Brent M. Peyton* **and W. G. Characklis**
NSF Center for Interfacial Microbial Process Engineering, College of Engineering, Montana State University, Bozeman, Montana 59717

Received May 19, 1992/Accepted October 29, 1992

One of the least understood processes affecting biofilm accumulation is detachment. Detachment is the removal of cells and cell products from an established biofilm and subsequent entrainment in the bulk liquid. The goal of this research was to determine the effects of shear stress and substrate loading rate on the rate of biofilm detachment.

Monopopulation *Pseudomonas aeruginosa* and undefined mixed population biofilms were grown on glucose in a RotoTorque biofilm reactor. Three levels of shear stress and substrate loading rate were used to determine their effects on the rate of detachment. Suspended cell concentrations were monitored to determine detachment rates, while other variables were measured to determine their influence on the detachment rate. Results indicate that detachment rate is directly related to biofilm growth rate and that factors which limit growth rate will also limit detachment rate. No significant influence of shear stress on detachment rate was observed.

A new kinetic expression that incorporates substrate utilization rate, yield, and biofilm thickness was compared to published detachment expressions and gives a better correlation of data obtained both in this research and from previous research projects, for both mono- and mixed-population biofilms.
Key words: biofilm • shear stress • substrate loading • biofilm detachment • *Pseudomonas aeruginosa*

INTRODUCTION

A biofilm is a matrix of cells and cellular products attached to a solid surface or substratum. At the substratum, cells grow, reproduce, and produce extracellular polymers and other byproducts. Biofilms are found in most natural and industrial aquatic systems and account for much of the overall microbial activity in these systems. In streams and rivers, a large proportion of the microbial activity occurs in attached films. Wuhrmann[33] estimated 90% to 99.99% of the bacterial activity in shallow streams is associated with biofilms. This microbial activity is responsible for the transformation and degradation of natural and man-made organic compounds in the water.

In industrial systems, biofilms reduce heat transfer efficiency in heat exchange equipment[10] and reduce flow capacity in pipelines, leading to increased energy consumption and increased costs.[20] Biofilms also contribute significantly to other industrial water problems, including the negative effects of corrosion, oilfield reservoir plugging, and petroleum souring. In addition, biofilms influence drinking water quality deterioration,[16] and lead to contamination of computer chip components.[32] However, biofilms also provide positive opportunities in bioremediation of hazardous and toxic substances in ground and surface water treatment, as well as more traditional wastewater treatment. Biofilm and other immobilized cell reactors offer significant advantages in bioprocessing, because greater throughputs can be achieved without washing the organisms from the reactor.

The accumulation of a biofilm is the net result of various processes such as adsorption, desorption, attachment, microbial growth, and detachment.[11] This article focuses on the process of biofilm detachment and the identification of variables that influence detachment rates. Biofilm detachment is the entrainment of cells and cell products from an existing biofilm into the bulk liquid and is the primary process that balances cell growth in a biofilm.

According to Bryers,[6] portions of a biofilm can be removed in any of the following ways: (1) erosion, (2) sloughing, (3) abrasion, (4) predator grazing, and (5) human intervention. Erosion is the continuous removal of small particles of biofilm and is presumed to be the result of shear forces exerted by moving fluid in contact with the biofilm surface. In contrast to erosion, sloughing is the detachment of very large portions of a biofilm and is an apparently random, discrete process. Sloughing often occurs in older, thicker biofilms, or when environmental conditions change rapidly. Abrasion is caused by collisions of solid particles with the biofilm. In fluidized-bed bioreactors, abrasion can be the dominant detachment process.[9] Detachment as a result of human intervention is the removal of a biofilm by chemical or physical means. Predator grazing, although not strictly a detachment process, is the consumption of biofilm mass by larger organisms such as protozoa, snails, worms, and insects. The focus of this study, and the most commonly encountered detachment process, is erosion.

The prediction of detachment rates has been a priority in understanding biofouling in drinking water distribution

* To whom all correspondence should be addressed at Battelle, Pacific Northwest Laboratories, Battelle Boulevard, Richland, WA 99352.

CCC 0006-3592/93/070728-08

pipelines. In each of these industries, detached biomass reduces final product quality and/or increases operating costs. Biofilms in drinking water distribution systems may harbor pathogenic organisms.[15] Detachment of these organisms and entrainment in the bulk liquid can result in failure to meet drinking water quality standards.

In the paper industry, detachment of macroscopic biofilm particles results in defects in the paper that can lower product value and reduce the strength of the unfinished paper. The resulting reduction in paper strength leads to expensive downtime when the paper sheets tear.

In oilfield injection water pipelines, increased biomass detachment accelerates fouling of preinjection filters, and may plug the formation itself. This results in more frequent maintenance or replacement of the filters, while formation plugging around an injection well results in decreased injection rates or higher injection pressure.

For all of these industries, decreasing biofilm detachment rates would reduce operational costs and/or improve product quality. An experimental program was completed to determine the influence of two important variables, shear stress and substrate loading rate, on the rate of biofilm detachment and to determine a mathematical expression describing detachment rates.

For computer simulation of biofilm accumulation in both laboratory and industrial systems, a mathematical expression for each biofilm process is required. Numerous expressions have been proposed for calculating the rate of biofilm detachment (Table I). While each has given reasonable results for the specific experimental application, none are general enough to extrapolate to other environmental conditions. The abundance of detachment rate equations partially reflects the failure of any one expression to model the detachment rate over a wide range of conditions. The variables previously incorporated into biofilm detachment expressions include the following: areal biomass density, $X_f (M\ \mathrm{L}^{-2})$, volumetric biomass density, $\rho_f (M\ \mathrm{L}^{-3})$, biofilm thickness, $L_f(\mathrm{L})$, shear stress, $\tau(M\ \mathrm{L}^{-1}\ t^{-2})$, and specific growth rate, $\mu\ (t^{-1})$. In this article, a detachment rate expression is proposed that incorporates the substrate utilization rate, $R_u\ (M\ \mathrm{L}^{-2}\ t^{-1})$, the yield coefficient, $Y_{x/s}\ (M\ M^{-1})$, and the biofilm thickness. The expression is applied to both monopopulation and mixed-population biofilm detachment and is statistically compared with other reported detachment expressions.

Table I. Survey of reported detachment rate expressions.

Eq. #	Reported detachment rate expression $R_d\ [=]\ M\ \mathrm{L}^{-2}\ t^{-1}$	Reference
(1)	$k_d X_f^2$	5, 27
(2)	$k_d \rho_f L_f \tau^{0.58}$	21
(3)	$k_d \rho_f L_f^2$	31
(4)	$L_f(k_d' + k_d'' \mu)$	25
(5)	$k_d \rho_f L_f = k_d X_f$	7, 14, 22
(6)	$k_d \rho_f \tau$	4

Modeling

An expression for calculating the detachment rate was derived[19] from an empirical modification of the biomass material balance on a biofilm reactor [Eq. (7)].

$$V \frac{dX_1}{dt} = Q(X_i - X_1) + \mu X_{1V} + R_d A - R_a A \qquad (7)$$

Eq. (7) can be simplified by the following assumptions appropriate to this article: (1) a sterile influent ($X_i = 0$); (2) the attachment rate is much lower than the detachment rate ($R_a \ll R_d$); (3) the short reactor residence time, 15 minutes, renders growth in suspension negligible ($\mu X_l V \ll R_d A$); and (4) the reactor is at pseudo–steady state with regard to the effluent biomass concentration ($VdX_l/dt \ll R_d A$). Thus, Eq. (7) reduces to

$$R_d = \frac{Q}{A} X_1 \qquad (8)$$

Eq. (8) indicates that detachment rate is proportional to effluent suspended biomass concentration. The dependence of detachment rate on substrate utilization rate can be established through the definition of biomass yield. At steady state, in a biofilm reactor,

$$(X_1 - X_i)_{ss} = (S_i - S_1)_{ss} Y_{x/s} \qquad (9)$$

For a sterile influent ($X_i = 0$), combining Eqs. (8) and (9) gives Eq. (10) which shows that the steady-state detachment rate is proportional to substrate utilization rate, R_u, with the proportionality coefficient equal to the observed biomass yield.

$$R_{d_{ss}} = \frac{Q}{A}(S_i - S_1) Y_{x/s} = R_u Y_{x/s} = R_p \qquad (10)$$

Eq. (10) is also the biomass production rate (R_p) and determines the upper bound on the detachment rate for a given set of environmental conditions. However, Eq. (10) does not describe the detachment rate at unsteady state.

For description of detachment rates at both steady and unsteady state, an empirical modification to Eq. (10) is proposed. Detachment rate has been expressed by others as a first order function of biofilm thickness.[7,14,21,22,25] Film thickness is a fundamental variable, is easy to monitor on a routine basis, and has been used in a mechanistic detachment model.[26] It is proposed that the detachment rate expression should be proportional to the product of the substrate utilization rate, biomass yield, and biofilm thickness:

$$R_d = k_d \frac{Q}{A}(S_i - S_1) Y_{x/s} L_f \qquad (11)$$

A comparison of Eq. (10) and Eq. (11) shows that the detachment rate is a function of the biomass production rate, as theoretically it should be.

MATERIALS AND METHODS

Organism

A pure culture of *Pseudomonas aeruginosa* was used in this experimental program. The species is a Gram-negative, motile, facultative aerobe, capable of denitrification. Separate vials of the stock culture were maintained in glycerol at −40°C to insure a reproducible inoculum. The *Ps. aeruginosa* strain is a known biofilm former[1] for which growth kinetic and stoichiometric coefficients have been determined previously.[23]

Media

Bacteria were grown aerobically on a defined salts medium with glucose as the sole carbon and energy source. The composition of the various media, as delivered to the reactor, are given in Table II. Concentrated micronutrient solutions were prepared in 11 L Nalgene bottles and autoclaved for 4 hours at 121°C. After autoclaving, 20 mL of sterile concentrated glucose solution was added to each micronutrient bottle to give a final glucose concentration of 500 g m^{-3}. Concentrated phosphate buffer solution was prepared in 3.5-L glass containers and autoclaved for 1 hour. Dilution water consisted of distilled water filtered through two 0.2-μm cartridge filters (Gelman). The concentrated micronutrient solution and concentrated buffer solution were mixed with dilution water immediately prior to entering the biofilm reactor. Micronutrient flow rates were adjusted to give the desired influent concentration of either 0.8, 4.0, or 7.2 g glucose carbon (GC) m^{-3}. The pH was buffered at 6.7 ± 0.02 throughout the experimental series.

Biofilm Reactor

A RotoTorque biofilm reactor (Fig. 1) was used because it permits quantitative monitoring and control of shear stress independent of the flow rate through the reactor. The reactor includes 12 removable slides for direct sampling of the biofilm. Draft tubes bored in the inner drum provide good mixing, so the bulk liquid may be analyzed as a continuous-flow stirred-tank reactor (CFSTR). The RotoTorque has a wetted surface area of 0.186 m^2 and an operating volume of 0.595 L (5.95×10^{-4} m^3). The temperature, pH, rotational speed, and torque were monitored with a laboratory interface (SCI Technologies, Bozeman, MT). These readings were continuously logged by computer. The reactor temperature was maintained at 20 ± 0.1°C with a water bath (Neslab, Portsmouth, NH).

Table II. Media composition entering RotoTorque reactor. All units in g m^{-3}.

	Inlet glucose carbon		
	0.8	4.0	7.2
NH_4Cl	0.72	3.6	6.5
$MgSO_4 \cdot 7H_2O$	0.2	1.0	1.8
$(NH_4)_6Mo_7O_{24} \cdot 4H_2O$	0.0001	0.0005	0.0009
$ZnSO_4 \cdot 7H_2O$	0.01	0.05	0.09
$MnSO_4 \cdot H_2O$	0.0008	0.004	0.0072
$CuSO_4 \cdot 5H_2O$	0.0002	0.001	0.0018
$Na_2B_4O_7 \cdot 10H_2O$	0.0001	0.0005	0.0009
$FeSO_4 \cdot 7H_2O$	0.0112	0.056	0.1008
$(HOCOCH_2)_3N$	0.04	0.2	0.36
$CaCl_2$	0.003	0.015	0.027
Na_2HPO_4	95.5	95.5	95.5
KH_2PO_4	102.0	102.0	102.0

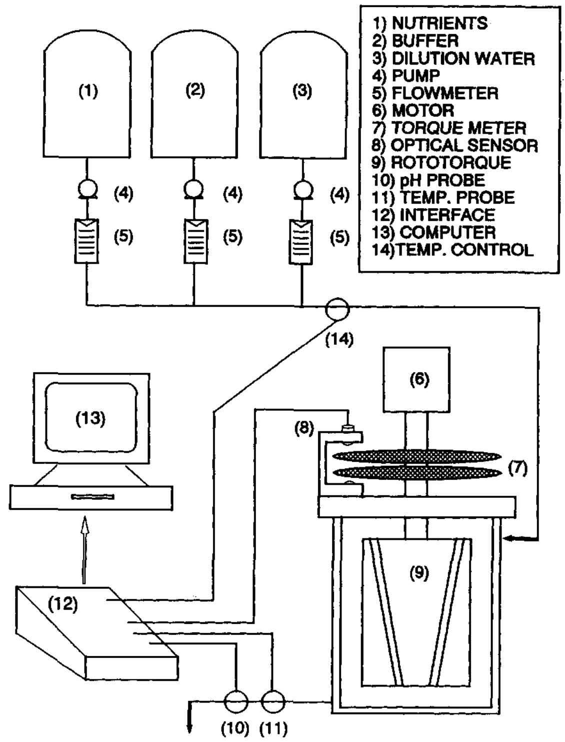

Figure 1. Experimental apparatus including the RotoTorque.

A torque transducer mounted on the drive shaft between the reactor and the motor was continuously monitored to record changes in frictional resistance. Rotational speed was maintained at 200 ± 0.3, 302 ± 0.5, or 400 ± 0.6 rpm, and was measured by optically monitoring a rotating gap in the torque transducer. The reactor was operated with a residence time of 0.25 hours ($D = 4$ h^{-1}), minimizing the effects of cellular growth in suspension.

Start-Up Protocol

The RotoTorque and tubing were autoclaved for 0.5 hours at 121°C and allowed to cool. After attaching the glucose/micronutrient, phosphate buffer, and dilution water tubes, the reactor was filled by pumping in a 1 : 1 : 10 mixture of the three solutions, respectively. Once the reactor was full, the flow was stopped and 0.5 mL of the *Ps. aeruginosa* stock culture (10^{19} cells m^{-3}) was introduced into the reactor. The RotoTorque was operated in batch mode at 200 rpm for 24 hours, at which point liquid flow was initiated and the rotational speed was set to the desired value. This time was defined as the experimental time zero. The phosphate buffer volumetric flow rate was constant at 24 mL h^{-1} (2.4×10^{-5} m^3 h^{-1}) throughout all experiments. The glucose/micronutrient solution volumetric flow rate was adjusted to give the desired influent glucose concentration. The flow rate of the dilution water was adjusted for a total volumetric flow rate of 2382 mL h^{-1} (2.382×10^{-3} m^3 h^{-1}).

Sampling and Analytical Methods

Biofilm thickness was measured optically with an Olympus CH-2 microscope at eight locations on a removable slide by the method of Bakke and Olsson.[3] The areal density of the biofilm was determined by scraping 0.0017 m^2 from a removable slide into a preweighed aluminum pan. The sample dried overnight and was weighed again to determine dry mass. The volumetric density was calculated by dividing the areal density by the average biofilm thickness determined from the same slide. Effluent-suspended cell concentrations were determined by direct counting according to the method of Hobbie et al.[13] Cells were stained with Hoechst 33342 and counted using an image analysis system (American Innovisions software and an Olympus BH-2 microscope). Glucose concentration was measured spectrophotometrically using a modification of the Sigma 510 enzymatic glucose analysis procedure. Statistical analyses were performed using the regression and analysis of variance (ANOVA) procedures in the computer software package MSUSTAT.[17]

RESULTS

A 3^2 factorial experimental design[18] was used to determine the effects on biofilm detachment rate of substrate loading rate and shear stress, each at three levels. The three rotational speeds were 200, 300, or 400 rpm corresponding to shear stresses of 1.44, 2.20, and 2.97 N m^{-2}, respectively. Although shear stress was continuously monitored, no change in shear stress was observed during the course of an experiment. The influent glucose carbon concentration was adjusted to either 0.8, 4.0, or 7.2 g GC m^{-3}, giving substrate loading rates, R_L, of 0.0102, 0.0512, and 0.0922 g GC m^{-2} h^{-1}, respectively.

Table III gives the steady-state detachment rate and number of experiment replications at each condition. Steady state was defined as the average time required to reach a constant biofilm thickness. For these experiments steady state was defined as $t > 140$ hours.

Each replication in Table III is a separate, independent experiment, with 12 experiments performed altogether. An advantage of this design is the ability to distinguish the main effects of each factor (shear stress or substrate loading rate) and any possible interactive effects between the two. Bartlett's test for checking the assumption of constant variance was performed with a null hypothesis that all variances were equal. An observed P-value of 0.042, although not much different from 0.05, indicates that all the variances were possibly not statistically equivalent at the 95% confidence level. It can be seen that the second experiment at 400 rpm and a loading rate of 0.0512 g GC m^{-1} h^{-1} did indeed have a higher standard error than the other experiments.

Table III. Statistical experimental design.

Rotational speed	Substrate loading (10^{-3} g GC m^{-2} h^{-1}) 10.2	51.2	92.2
200 rpm	1.64 ± 0.18	6.97 ± 0.70	17.25 ±[a]
300 rpm	0.68 ± 0.07	6.54 ± 0.65	16.99 ± 0.48
		7.81 ± 0.48	
		5.86 ± 0.46	
400 rpm	2.02 ± 0.24	6.38 ± 0.58	15.27 ± 0.78
		5.29 ± 1.51	

[a] No standard error because of contamination.

Entries indicate mean steady-state detachment rate, R_{dss} (10^{-3} g CC m^{-2} h^{-1}), and standard error of individual experiments at the specified conditions.

As the biofilm accumulates, substrate utilization, biofilm thickness, and detachment rate increase until steady state is reached. Average steady-state substrate utilization and film thickness values are given in Table IV. Measured detachment rates are plotted as a function of shear stress and substrate loading rate in Figures 2a and 2b. Figure 2a indicates that different, though constant, shear stress had no significant influence on the steady-state detachment rate. In Figure 2b, on the other hand, it is clear that detachment rate varied with the substrate loading rate. These observations are supported by standard analysis of variance calculations (Table V). The P-values in the last column of Table V indicate the extent to which the data agree with the corresponding null hypothesis. A low P-value signifies that the data discredit the null hypothesis, where the null hypothesis is that the true value of the detachment rate is the same at all three values of the independent variable. Over the range of variables tested, only the substrate loading rate (P, ≤ 0.0001) had a significant influence on detachment rate. Shear stress (P, 0.2644) had no significant effect and there was no interactive effect (P, 0.5842).

To further define the role of shear stress, Eqs. (2) and (6) (Table I) were rewritten in a more general form, given

Table IV. Observed steady state values of R_u [Eq. (10)] and L_f for three substrate loading rates, R_L.

R_L (10^{-3} g GC m^{-2} h^{-1})	R_U (10^{-3} g GC m^{-2} h^{-1})	L_f (10^{-6} m)
10.2	5.89 ± 0.29	5.88 ± 0.51
51.2	44.32 ± 0.32	17.98 ± 0.75
92.2	81.23 ± 2.03	31.93 ± 1.79

Values are means ± standard error for replicate experiments and measurements.

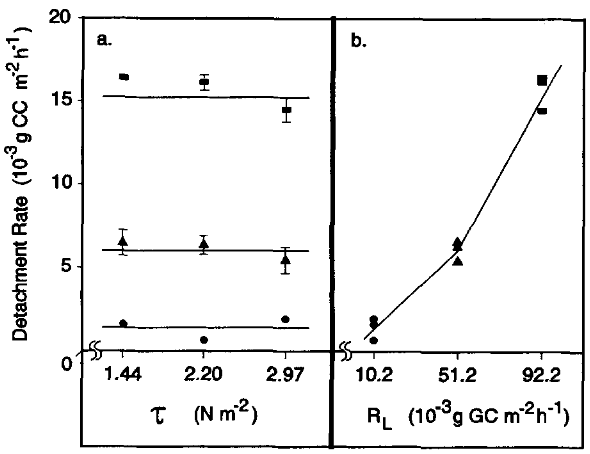

Figure 2. The influence of shear stress (τ) and substrate loading rate (R_L) on cell carbon (CC) detachment rate of a monopopulation *Ps. aeruginosa* biofilm.

Table V. Analysis of variance of cellular detachment rate as a function of the shear stress and the substrate loading rate.

Source	*DF*	SS	MS	*F*-value	*P*-value
τ	2	8.7553	4.3777	1.41	0.2644[a]
R_L	2	366.09	183.05	58.96	<0.0001[a]
$\tau * R_L$	4	8.9971	2.2493	0.72	0.5842[b]
Residual	23	71.405	3.1045		

[a] Null hypothesis is that the true mean detachment rate is the same at all three levels of the independent variable, shear stress, or substrate loading rate.

[b] Null hypothesis is that there is no interaction between shear stress and substrate loading rate affecting the mean detachment rate.

by the following:

$$R_d = k_d \rho_f L_f \tau^n \quad (12)$$

$$R_d = k_d \rho_f \tau^n \quad (13)$$

The equations were linearized by taking logarithms, and then n was estimated by least squares linear regression analysis. Exponent values (n) on shear stress were estimated from the data of the present study alone and in combination with data from other experimental investigations with monopopulation *Ps. aeruginosa* biofilms.[24,28,29] The mixed population data of Trulear, previously evaluated by Rittman[21] resulting in Eq. (2), were also analyzed. The results are given in Table VI. From the data obtained in this research, the estimated exponent on shear stress in Eq. (12) was −0.27, a value statistically indistinguishable from zero. The associated 95% confidence interval (−1.59, 1.05) contains both $n = 0.58$ [Eq. (2)] and $n = 1.0$ [Eq. (6)], values proposed by other authors. When all monopopulation data were combined, the estimated value of $n = 0.55$ [Eq. (12)] was similar to the proposed value of $n = 0.58$ [Eq. (2)]. The exponent on shear stress in Eq. (12) for the mixed-population data set was −0.64.

Table VI. Dependence of detachment rate on shear stress. The influence of shear stress was determined as an exponent on shear stress from Eqs. (12) and (13).

	n [Eq. (12)]	SE(*n*) [Eq. (12)]	*n* [Eq. (13)]	SE(*n*) [Eq. (13)]
Proposed value and ref.	0.58 (ref. 21)	—	1.0 (ref. 4)	—
Ps. aeruginosa, this investigation	−0.27	0.64	−0.43	0.89
Ps. aeruginosa, this investigation combined with data from refs. 24, 27, and 28	0.55	0.12	−0.18	0.20
Mixed culture, ref. 26	−0.64	0.11	0.52	0.13

Trulear and Characklis[27] original detachment data with shear stress are replotted in Figure 3. Figure 3 illustrates detachment rate as a function of the shear stress as calculated from the measured torque. The squared correlation coefficient (r^2) of 0.00038 between detachment rate and shear stress suggests no linear relationship.

The detachment expressions were compared by using the squared correlation coefficient (r^2) associated with each detachment expression calculated separately for the data of this investigation, the combined data set, and the mixed population data set (Table VII). Confidence intervals (95%) were calculated for the correlation coefficients for all three data sets by Fisher's arctangent method. The confidence intervals for the correlation coefficient of Eq. (11) do not overlap with those of either Eqs. (2) or (6), indicating that the improvement in Eq. (11), over Eqs. (2) or (6) is statistically significant.

Figures 4 and 5 show plots of the observed versus predicted detachment rates based on Eq. (11) for the combined data set and the mixed-population data set, respectively.

DISCUSSION

Our experiments, in which each biofilm was grown under a different but constant shear stress indicate that: (1) within

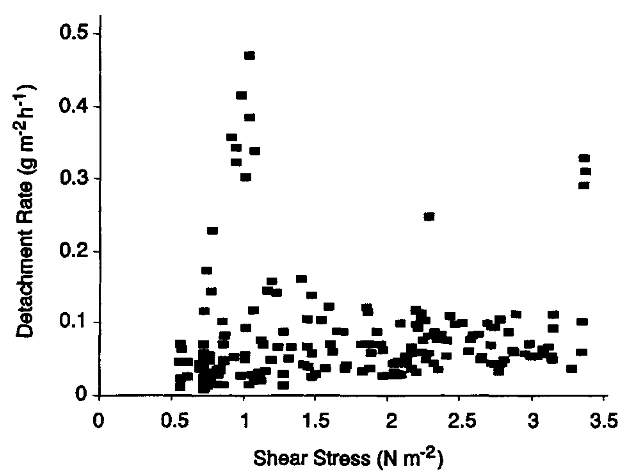

Figure 3. Mixed-population suspended solids detachment rates[27] do not correlate with measured shear stress.

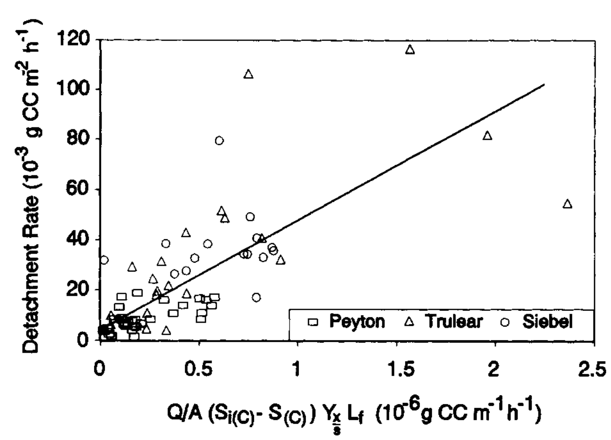

Figure 4. Monopopulation *Ps. aeruginosa* cell carbon detachment rates from this research and other experimental investigations[24,28] combined are linearly related to the proposed detachment rate expression and give a correlation coefficient of 0.59.

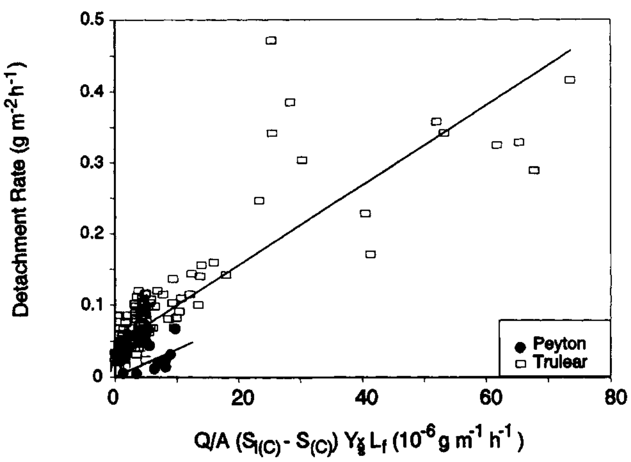

Figure 5. Mixed-population suspended solids detachment rates from this research and from Trulear and Characklis[27] give squared correlation coefficients of 0.58 and 0.73, respectively, for the proposed detachment rate expression [Eq. (11)].

the range of environmental conditions tested, shear stress had no significant influence on the detachment rate; and (2) the product of substrate utilization rate, yield, and biofilm thickness gave the best description of the detachment rate. According to the squared correlation coefficients, shown in Table VII, the models which are growth dependent [Eqs. (3), (4), and (11)] are better predictors of detachment rate than Eqs. (2) and (6) which are dependent on shear stress. Eq. (11) gives a statistically better correlation than either Eqs. (2) or (6).

Shear Stress

The results indicate that over the range of 0.5 to 3.4 N m^{-2}, there was no significant influence of shear stress on the cellular detachment rate, for either mono- or mixed populations (Fig. 2a and Table IV for *Ps. aeruginosa* biofilms; Fig. 3 for mixed-population biofilms). This observation is limited to systems under constant or gradually changing shear stress. In contrast, Bakke[2] has shown that rapid increases in shear stress can cause transient increases in detachment rates. Bakke's research revealed, however, that detachment rate returned to its original level within five reactor residence times, even at the higher shear stress, indicating that the biofilm quickly adapts to a different shear stress. Rapid decreases in shear stress did not affect the detachment rate. In light of these observations, a detachment rate expression that incorporates the rate of change of the shear stress, rather than the shear stress itself, may be more appropriate [Eq. (14)]:

$$R_d = R_{de} + R_{d\Delta\tau}$$

$$\text{where } R_{d\Delta\tau} = \begin{bmatrix} k_d \dfrac{d\tau}{dt}, & \dfrac{d\tau}{dt} > 0 \\ 0, & \dfrac{d\tau}{dt} \leq 0 \end{bmatrix} \tag{14}$$

Eq. (14) incorporates the continuous detachment rate as a result of erosion [Eq. (11) for example] and the transient detachment rates which result from increases in shear stress. Eq. (14) could be easily implemented in computer models and may better reflect the effects of shear stress on biofilm detachment.

Some influence of the bulk liquid velocity on detachment may be hypothesized. As the liquid velocity at the biofilm–bulk liquid interface increases, the shear forces exerted on the biofilm increase while, at the same time, mass transfer resistance decreases. If detachment rate is

Table VII. Squared correlation coefficient (r^2) of reported detachment expressions.

Eq. #	Detachment rate expression R_d [=] M L^{-2} t^{-1}	Data from this investigation	Data from this investigation combined with refs. 24, 27, and 28	Mixed culture data from ref. 26	Rank
(11)	$k_d Q/A(S_i - S_j) Y_{X/S} L_f$	0.56	0.59	0.73	1
(4)	$L_f(k_d' + k_d'' \mu)$	0.37	0.20	0.42	2
(3)	$k_d \rho_f L_f^2$	0.43	0.42	0.13	3
(1)	$k_d X L_f^2$	0.22	0.26	0.27	4
(5)	$k_d \rho_f L_f$	0.25	0.24	0.24	5
(2)	$k_d \rho_f L_f \tau^{0.58}$	0.025	0.23	0.060	6
(6)	$k_d \rho_f \tau$	0.028	0.026	0.021	7

Equations are ranked by average r^2 for three columns; 1 is highest rank.

independent of shear stress, but is dependent on mass transfer of substrate to the biofilm, then there will be a flow velocity region (perhaps at the lower end of the turbulent flow range) where detachment rate increases with increasing flow velocity. However, such an increase in detachment rate with increasing fluid velocity would be the result of increased substrate removal by the biofilm and not a direct result of increased shear stress at the biofilm interface. If shear stress does have some effect on the detachment rate, the influence is insignificant when compared to that of the substrate utilization rate.

Substrate Utilization Rate

The accumulation of a biofilm is the net result of processes that produce biomass and processes that remove it. The accumulation continues until the biofilm reaches steady state, at which point biomass production is balanced primarily by biomass detachment. Thus, material balance considerations alone establish the biomass production rate [Eq. (10)] as the upper limit for a sustainable detachment rate. Eq. (11) incorporates this inherent substrate dependence of the biofilm detachment rate into an expression that predicts both steady- and unsteady-state detachment rates for both monopopulation and mixed-population biofilms.

Eq. (11) predicts high detachment rates during periods of high growth rates, i.e., high substrate utilization rates. This association has been observed previously.[8,25] The relationship between the more fundamental variables, $\bar{\mu}$ and X_{fc}, and the substrate utilization rate can be shown by a cell balance on the biofilm:

$$A\frac{dX_{fc}}{dt} = \bar{\mu}X_{fc}A + R_aA - R_dA \qquad (15)$$

At steady state with a negligible attachment rate, the cell balance reduces to Eq. (16).

$$R_{\text{dss}} = \bar{\mu}X_{fc} \qquad (16)$$

Equating Eqs. (16) and (10) yields:

$$\bar{\mu}X_{fc} = \frac{Q}{A}(S_i - S_1)Y_{x/s} \qquad (17)$$

Eq. (17) indicates that measurement of the influent and effluent substrate concentrations in the bulk liquid, and an estimate of the yield, can be substituted for values of the more difficult to measure $\bar{\mu}$ and X_{fc} in the characterization of steady-state detachment rates.

By substituting Eq. (17) into the proposed detachment expression [Eq. (11)], it can be shown that Eq. (11) is equivalent to:

$$R_d = k_d\bar{\mu}\rho_{fc}L_f^2 \qquad (18)$$

Eq. (18) is a special case of a mechanistic detachment model.[26]

Eq. (4) was proposed by Speitel and DiGiano[25] to reflect high detachment rates observed during periods of high growth rate. It is interesting to note that Speitel and DiGiano report some dependence of the growth-associated detachment rate coefficient, k_d'' (M L^{-3}), on the type of substrate used. Eq. (11) is also dependent on the type of substrate, because the yield coefficient will be influenced by substrate properties (e.g., free energy of oxidation). A substrate which is more difficult to metabolize or provides less energy for producing biomass will result in lower detachment rates for the same substrate conversion rate.

These results have significance to a wide variety of industries. In drinking water distribution systems, it is believed that detachment from biofilms results in high heterotrophic plate counts (HPC) and high coliform counts even in systems with a significant chlorine residual.[30] It has also been found that lowering the assimilable organic carbon (AOC) will give lower coliform and HPC counts.[15] These observations are consistent with the data and analysis presented here. A lower AOC concentration is equivalent to a lower substrate loading rate and, subsequently, a lower substrate utilization rate. This would result in less detachment of coliforms and HPC from the biofilm found in the distribution systems. In the semiconductor industry, it is common practice to lower the organic carbon concentration with synthetic scavengers, thus reducing the substrate available for attached microbial growth and subsequent detachment.[12]

In oilfield injection systems, biomass that detaches from the preinjection pipelines is either removed by filtration or is injected into the formation. In either case, increased detachment leads to increased operation and maintenance costs. Eq. (11) suggests that lowering the AOC or electron acceptor concentration in these systems would extend filter life and reduce the need for biocide treatments. In the absence of preinjection filters, less biomass would be injected downhole, which would result in less acid cleaning of injection wells.

CONCLUSIONS

The results from this investigation, within the range of variables tested, have led to the following conclusions:

1. The cellular detachment rate is dependent on the cellular production rate.
2. An expression which incorporates substrate utilization rate, yield coefficient, and biofilm thickness gives better description of detachment rates than any previously proposed models.
3. Different, though constant, shear stress had no significant influence on the detachment rate.

The authors gratefully acknowledge financial support from Conoco, Inc., and the National Science Foundation Engineering Research Centers Program. Dr. Philip Stewart and Dr. Martin Hamilton kindly provided editorial comments. The authors give special thanks to Dr. Robert M. Huddleston, Conoco, Inc., for his time and support. This article is dedicated in loving memory to Dr. Bill Characklis who passed away in June 1992.

NOMENCLATURE

A	reactor area (L^2)
D	dilution rate (t^{-1})

k_d detachment rate coefficient (expression dependent units)
k_d' detachment rate coefficient (M L^{-3} t^{-1})
k_d'' detachment rate coefficient (M L^{-3})
L_f biofilm thickness (L)
n exponent on shear stress, Eqs. (12) and (13) (−)
p probability (−)
Q volumetric flow rate (L^3 t^{-1})
r^2 squared correlation coefficient (−)
R_a attachment rate (M L^{-2} t^{-1})
R_d detachment rate (M L^{-2} t^{-1})
R_{de} detachment rate as a result of erosion (M L^{-2} t^{-1})
R_{dss} steady-state detachment rate (M L^{-2} t^{-1})
$R_{d\Delta\tau}$ detachment rate as a result of a change in shear stress (M L^{-2} t^{-1})
R_L substrate loading rate (M L^{-2} t^{-1})
R_p biomass production rate (M L^{-2} t^{-1})
R_u substrate utilization rate (M L^{-2} t^{-1})
S_i influent substrate concentration (M L^{-3})
S_l substrate concentration (M L^{-3})
t time (t)
V reactor volume (L^3)
X biomass concentration (M L^{-3})
X_f biofilm areal mass density (M L^{-2})
X_{fc} biofilm areal cell density (M L^{-2})
X_i influent biomass concentration (M L^{-3})
X_l bulk liquid biomass concentration (M L^{-3})
$Y_{x/s}$ observed biomass yield coefficient (M M^{-1})

Greek letters

ρ_f biofilm volumetric mass density (M L^{-3})
ρ_{fc} biofilm volumetric cell density (M L^{-3})
μ specific growth rate (t^{-1})
$\bar{\mu}$ average specific growth rate in the biofilm (t^{-1})
τ shear stress (M L^{-1} t^{-2})

References

1. Bakke, R. 1986. Biofilm detachment, Ph.D. thesis, Montana State University, Bozeman, MT.
2. Bakke, R., Olsson, P.Q. 1986. Biofilm thickness measurements by light microscopy, J. Microbial Meth. **5**: 93.
3. Bakke, R., Trulear, M.G., Robinson, J.A., Characklis, W.G. 1984. Activity of *Pseudomonas aeruginosa* in biofilms: Steady state. Biotechnol. Bioeng. **26**: 1418–1424.
4. Bakke, R., Characklis, W.G., Turakhia, M.H., Yeh, An-I. 1990. Modeling a monopopulation biofilm system: *Pseudomonas aeruginosa,* pp. 487–520. In: W.G. Characklis and K.C. Marshall (eds.), *Biofilms.* Wiley, New York.
5. Bryers, J.D. 1984. Biofilm formation and chemostat dynamics: Pure and mixed culture considerations. Biotechnol. Bioeng. **26**: 948.
6. Bryers, J.D. 1987. Biologically active surfaces: Processes governing the formation and persistence of biofilms. Biotechnol. Prog. **3**: 57.
7. Chang, H.T., Rittmann, B.E. 1987. Mathematical modeling of biofilm on activated carbon. Environ. Sci. Technol. **21**: 273–279.
8. Chang, H.T., Rittmann, B.E. 1988. Comparative study of biofilm shear loss on different adsorptive media, J. WPCF **60**: 362–368.
9. Chang, H.T., Rittmann, B.E., Amar, D., Heim, R., Ehlinger, O., Lesty, Y. 1991. Biofilm detachment mechanisms in a liquid-fluidized bed. Biotechnol. Bioeng. **38**: 499–506.
10. Characklis, W.G., Bryers, J.D., Trulear, M.G., Zelver, N. 1980. In: J.F. Garey et al. (eds.), Biofouling development and its effects on energy losses: A laboratory study, condenser biofouling control. Ann Arbor Science Publishers, Inc., Ann Arbor, MI, p. 49.
11. Characklis, W.G. 1990. Biofilm Processes, pp. 195–231. In: W.G. Characklis and K.C. Marshall (eds.), Biofilms. Wiley, New York.
12. Collentro, W.V. 1986. Synthetic organic scavengers. Ultrapure Wat. **3**: 51–54.
13. Hobbie, J.E., Daley, R.J., Jasper, S. 1977. Use of nuecleopore filters for counting bacteria by fluorescence microscopy. Appl. Environ. Microbiol. **35**: 858–862.
14. Kreikenbohm, R., Stephan, W. 1985. Application of a two-compartment model to the wall growth of *Pelobacter acidigallici* under continuous culture conditions. Biotechnol. Bioeng. **27**: 296–301.
15. LeChevallier, M.W., Babcock, T.M., Lee, R.G. 1987. Examination and characterization of distribution system biofilms. Appl. Environ. Microbiol. **53**: 2714–2724.
16. LeChevallier, M.W., Schulz, W., Lee, R.G. 1991. Bacterial nutrients in drinking water. Appl. Environ. Microbiol. **57**: 857–862.
17. MSUSTAT Version 3.2. 1986. Available through RDI, Montana State University, Bozeman, MT 59715.
18. Petersen, R.G. 1985. Design and analysis of experiments. Marcel Dekker, New York, pp. 112–124.
19. Peyton, B.M. 1992. Kinetics of biofilm detachment, Ph.D. thesis, Montana State University, Bozeman, MT.
20. Picologlou, B.F., Zelver, N., Characklis, W.G. 1980. Biofilm growth and hydraulic performance. J. Hydraulics Div. ASCE **106**: 733.
21. Rittmann, B.E. 1982. The effect of shear stress on biofilm loss rate, Biotechnol. Bioeng. **24**: 501–506.
22. Rittmann, B.E. 1989. Detachment from biofilms, pp. 49–58. In: W.G. Characklis and P.A. Wilderer (eds.), Structure and function of biofilms. Wiley, New York.
23. Robinson, J.A., Trulear, M.G., Characklis, W.G. 1984. Cellular reproduction and extracellular polymer formation by *Pseudomonas aeruginosa* in continuous culture. Biotechnol. Bioeng. **26**: 1409–1417.
24. Siebel, M.A. 1987. Binary population biofilms, Ph.D. thesis, Montana State University, Bozeman, MT.
25. Speitel, G.E. Jr., DiGiano, F.A. 1987. Biofilm shearing under dynamic conditions. J. Environ. Eng. ASCE **113**: 464.
26. Stewart, P. 1993. A model of biofilm detachment. Biotechnol. Bioeng. (to appear).
27. Trulear, M.G., Characklis, W.G. 1982. Dynamics of biofilm processes. J. WPCF **54**: 1288–1301.
28. Trulear, M.G. 1983. Cellular reproduction and extracellular polymer formation in the development of biofilms, Ph.D. thesis, Montana State University, Bozeman, MT.
29. Turakhia, M.H. 1986. The influence of calcium on biofilm processes, Ph.D. thesis, Montana State University, Bozeman, MT.
30. van der Wende, E., Characklis, W.G., Smith, D.B. 1989. Biofilms and bacterial drinking water quality. Wat. Res. **23**: 1313–1322.
31. Wanner, O., Gujer, W. 1986. A multispecies biofilm model. Biotechnol. Bioeng. **28**: 314–328.
32. White, D.C., Mittleman, M.W. 1990. Biological fouling of high purity waters: Mechanisms and consequences of bacterial growth and replication. Semiconductor Pure Water Conference, Santa Clara, CA.
33. Wuhrmann, K. 1971. Stream purification, p. 119. In: R. Mitchell (ed.), *Water pollution microbiology.* Wiley, New York.